ChemPubSoc Europe

DOI: 10.1002/chem.201504451

CHEMISTRY A European Journal Full Paper

Supramolecular Chemistry

Mechanochemical Encapsulation of Fullerenes in Peptidic Containers Prepared by Dynamic Chiral Self-Sorting and Self-Assembly

Marek Szymański[+],[a] Michał Wierzbicki[+],[a] Mirosław Gilski,[b, c] Hanna Jędrzejewska,[a] Marcin Sztylko,[a] Piotr Cmoch,[a] Aleksander Shkurenko,[d] Mariusz Jaskólski,*[b, c] and Agnieszka Szumna*[a]

Abstract: Molecular capsules composed of amino acid or peptide derivatives connected to resorcin[4]arene scaffolds through acylhydrazone linkers have been synthesized using dynamic covalent chemistry (DCC) and hydrogen-bond-based self-assembly. The dynamic character of the linkers and the preference of the peptides towards self-assembly into β-barrel-type motifs lead to the spontaneous amplification of formation of homochiral capsules from mixtures of different substrates. The capsules have cavities of around 800 Å^3 and exhibit good kinetic stability. Although they retain their dynamic character, which allows processes such as chiral self-sorting and chiral self-assembly to operate with high fidelity, guest complexation is hindered in solution. However, the quantitative complexation of even very large guests, such as fullerene C_{60} or C_{70}, is possible through the utilization of reversible covalent bonds or the application of mechanochemical methods. The NMR spectra show the influence of the chiral environment on the symmetry of the fullerene molecules, which results in the differentiation of diastereotopic carbon atoms for C_{70}, and the X-ray structures provide unique information on the modes of peptide–fullerene interactions.

Introduction

The chemical diversity and biocompatibility of peptides have stimulated intensive research on their applications as supramolecular building blocks in the field of artificial nanomaterials. Numerous examples of the application of peptide-based synthetic materials have been reported, including targeted drug delivery systems,[1] materials for regenerative medicine,[2] retroviral gene transfer, and the even capturing carbon dioxide from fuel gas.[3] However, relatively long peptidic or peptidomimetic sequences[4] or the presence of additional interacting groups are required to obtain predictable and functional 3D structures. Consequently, the practical applications of peptidic building blocks are often limited by their synthesis.[5] In this regard, the utilization of relatively easily available, modified, short peptides has proven to be more practical.[6] A promising but largely unexplored approach involves the combination of short peptides with dynamic covalent chemistry (DCC). This approach takes advantage of the natural tendency of peptides to self-assemble as well as of the reversible character of chemical reactions to amplify the formation of complex functional structures.[7] Dynamic structures based on peptides can also potentially benefit from the unique features of the DCC approach, such as the possibility of self-sorting, ligand-templating/complexation, and self-healing. However, they also present significant challenges, such as the need to strike a balance between kinetic and thermodynamic parameters, or the need to control the flow of energy to the system to cross various energy barriers.

In this paper we present the formation of new, dynamic, and yet highly stable peptidic capsules and show various ways to cross the energy barriers of covalent and noncovalent processes (reversible chemical reactions, self-assembly, and complexation). Our de novo designed capsules possess acylhydrazone linkers and peptides connected through their carbon termini, which results in enhanced kinetic and thermodynamic stability. On the other hand, high stability implies the existence of high energy barriers that hamper the complexation of guests. We show that the barriers can be surmounted by utilizing the re-

[a] *M. Szymański,[+] M. Wierzbicki,[+] H. Jędrzejewska, M. Sztylko, Dr. P. Cmoch, Prof. A. Szumna*
Institute of Organic Chemistry, Polish Academy of Sciences
Kasprzaka 44/52, 01-224 Warsaw (Poland)
E-mail: agnieszka.szumna@icho.edu.pl

[b] *Dr. M. Gilski, Prof. M. Jaskólski*
Faculty of Chemistry, A. Mickiewicz University
Umultowska 89b, 61-614 Poznan (Poland)
E-mail: mariuszj@amu.edu.pl

[c] *Dr. M. Gilski, Prof. M. Jaskólski*
Institute of Bioorganic Chemistry, Polish Academy of Sciences
Noskowskiego 12/14, 61-704 Poznan (Poland)

[d] *Dr. A. Shkurenko*
Institute of Physical Chemistry, Polish Academy of Sciences
Kasprzaka 44/52, 01-224 Warsaw (Poland)

[+] *These individuals contributed equally to this work.*

Supporting information for this article is available on the WWW under http://dx.doi.org/10.1002/chem.201504451.

versible character of covalent bonds or by mechanochemical methods. Although the mechanisms of chemical processes under extreme mechanical forces are still poorly understood, the high potential of mechanochemistry in controlling supramolecular and dynamic systems has recently been demonstrated.[8] We conclusively show the effective complexation of non-intuitive guest molecules, fullerenes C_{60} and C_{70}, inside our peptidic capsules and analyze the fullerene–peptide interactions.

Results and Discussion

Design and synthesis

We have previously demonstrated that short peptides can serve as building blocks for the dynamic formation of capsules, provided that they are properly pre-organized by, for example, connection to a macrocyclic skeleton.[9] The peptides are connected to the scaffolds by imine linkers through their nitrogen termini. However, an intrinsically low energy barrier for the imine formation/hydrolysis reaction precluded further applications of such capsules for complexation (under ambient conditions, the imine linkers were prone to disruption even by simple neutral molecules). A new generation of dynamic peptidic capsules has been designed by using the resorcin[4]arene scaffold **1**[10] and peptidic fragments **2a**–**3b** connected through acylhydrazones as dynamic linkages (Figure 1). The acylhydrazone linkers display an excellent balance between facile reversibility and stability, as suggested[11] and exploited by Sanders and co-workers.[12] Additionally, acylhydrazones are compatible with water and biological environments,[13] and their formation can be catalyzed under mild conditions in media of various pH.[14] It should be noted that simple aromatic acylhydrazones attached to the resorcinarene scaffold have been previously used for the formation of molecular capsules, however, not in a dynamic way.[15]

The peptide hydrazides **2a**–**3b** were synthesized by using the EDCI/OXYMA (EDCI = 1-ethyl-3-(3-dimethylaminopropyl)-carbodiimide, OXYMA = ethyl (hydroxyimino)cyanoacetate) peptide coupling strategy (see the Supporting Information). The reaction of **1** with peptide hydrazides **2a**–**3b** gave tetra-substituted acylhydrazones **4a**–**5b** in high yields (85–97%, Figure 1a). Control experiments were performed to verify the reversibility of the reaction under the conditions employed. When L-**4a** was mixed with L-**4b** and heated at 70 °C for 7 days, scrambling of the acylhydrazone fragments was observed, which indicates the reversibility of the reaction under such conditions (see Figures S24–S28 in the Supporting Information).

Isomerism

Acylhydrazones **4a**–**5b** have many possible isomers, including regioisomers, tautomers, and atropisomers. The isomerism originates from keto–enol and amide–iminol tautomerism and from *E*/*Z* isomerization of the double and partial double bonds at various positions. All the isomerization processes have been

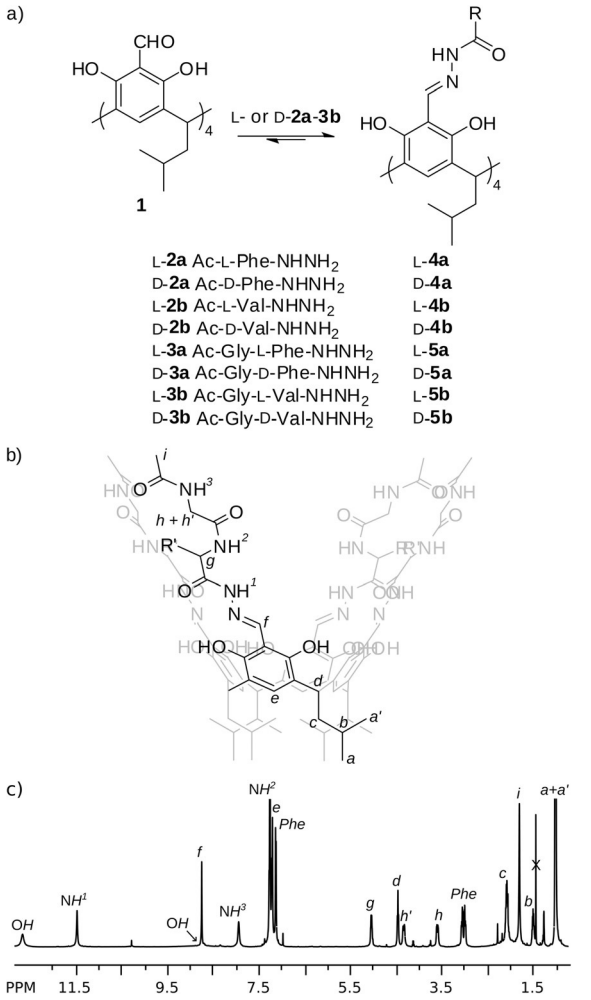

Figure 1. a) Synthesis of acylhydrazones **4a**–**5b**. b) Full chemical structure of a capsule hemisphere, with the atomic labelling scheme. The front arm is shown in black, the remaining ones, shown in perspective, are in gray. c) ^{1}H NMR spectrum of (L-**5a**)$_2$ ($CDCl_3$, 300 K, 600 MHz).

previously reported for analogous functional groups.[16] In the present case, the acylhydrazones **4a**–**5b** exhibit simple ^{1}H and ^{13}C NMR spectra in nonpolar solvents, consistent with the C_4 symmetry of the molecules, assuming single tautomeric forms in all arms (Figure 1c). Analysis of the ^{1}H–^{15}N and ^{1}H–^{13}C HSQC and HMBC spectra of **4a**–**5b** allowed us to determine the positions of the hydrogen atoms and thus to assign the specific tautomeric forms (see the Supporting Information). For all the products **4a**–**5b**, the resorcinol rings exist in the enol form and the acylhydrazone groups assume the amide form (Figure 1b). The X-ray crystal structures of **4b** and **5a** also confirmed that all the C_{ar}—OH bonds are of the same length, which indicates the enol form of the resorcinol rings. Note that the tautomeric form of the resorcin[4]arene skeleton in the case of acylhydrazones **4a**–**5b** is different from the keto–enamine form reported previously for peptidic capsules based on imine linkages.[10]

Self-assembly

The NMR spectra and X-ray structures confirm that all the synthesized peptidic acylhydrazones **4a**–**5b** form self-assembled capsular dimers in solution and in the solid state. The ROESY spectra of acylhydrazones **4a** and **4b** (amino acid derivatives) each show the ROE effect between the protons *f* and *h* (see Figures S5 and S10 in the Supporting Information). For acylhydrazones **5a** and **5b** (dipeptides), a ROE was observed between the protons *f* and *h*,*h*'' (see Figures S15 and S20). The proximity of these protons is consistent with the formation of self-assembled structures. Additionally, the diffusion coefficients observed for the present acylhydrazones are similar to the values reported for other dimeric capsules (see Table S1). All these findings strongly suggest that in solution the acylhydrazones exist as dimers.

The X-ray crystal structure of (D-**4b**)$_2$ confirms the formation of self-assembled dimers with two hemispheres interacting through hydrogen bonds between their peptide backbones (Figure 2a). The hydrogen-bonding motif involves the formation of four pairs of antiparallel strands, resembling the antiparallel β-sheet binding motif in a β-barrel (Figure 2c,e). The conformation of the peptidic chains also corresponds to typical Ramachandran angles of natural β-sheet structures ($\phi = -118.4^\circ$, $\psi = 107.2^\circ$). The interstrand hydrogen-bonded cycles are formed as 10-membered rings (orange motif). Notably, the binding motif is not fully complementary; the strands are grouped pairwise, with unmatched amide groups (Figure 2a), which act to bridge the paired-strands through the recruitment of hydrogen-bonded ethanol molecules.

The X-ray structure of (D,L-**5a**)$_2$ (Figure 2b) also confirms the formation of a dimeric self-assembled capsule. The binding motif also involves the formation of four antiparallel β-sheet "pairs of strands" (Figure 2d). However, an important difference between the binding motifs of capsules (D-**4b**)$_2$ and (D,L-**5a**)$_2$ is that in the latter case the interstrand pairing leads to the formation of 14-membered rings (Figure 2d,e, blue motif). The second amino acid residue in each strand (Gly) plays a less defined role as it interconnects the "pairs of strands" or mediates interactions with other capsules and solvent molecules in the crystal. It is important to note that although the sample was crystallized from a racemate and the space group is centrosymmetric, each individual capsule contains only homochiral hemispheres. This strongly suggests a preference towards the formation of homochiral dimers by the dipeptidic acylhydrazones.

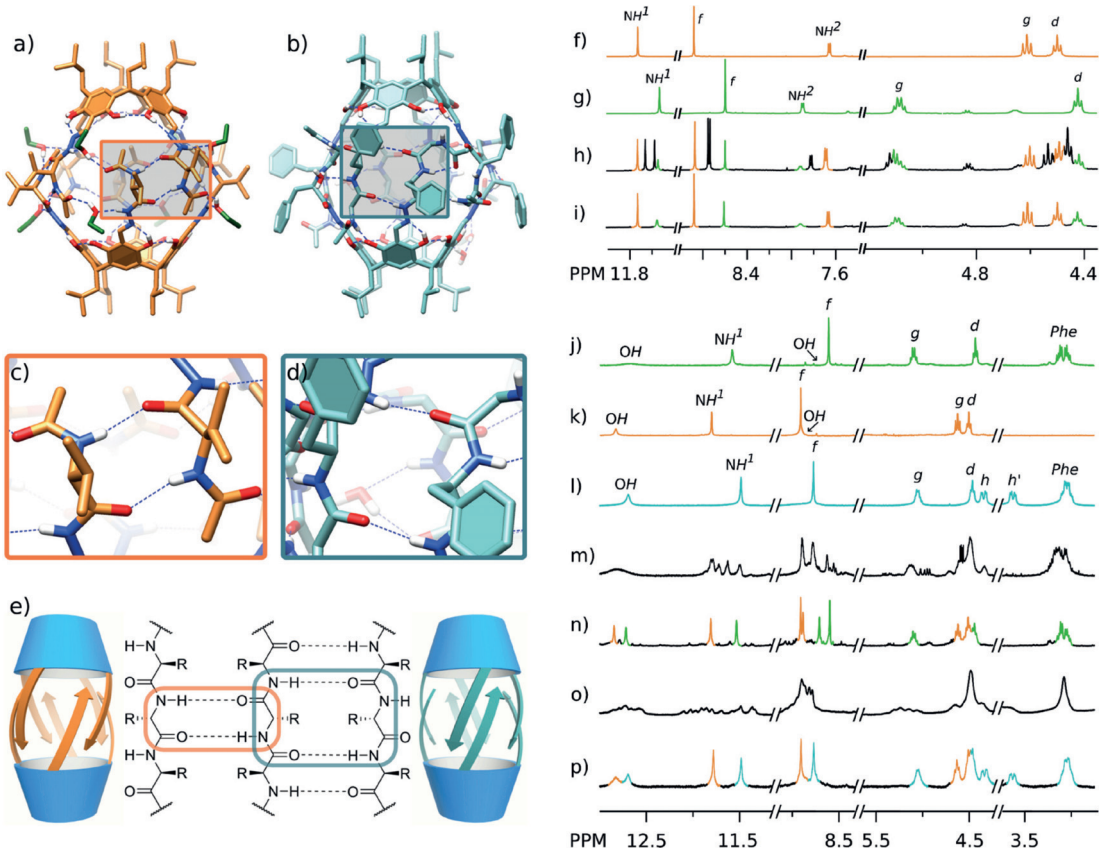

Figure 2. X-ray crystal structures of a,c) (D-**4b**)$_2$ and b,d) (D,L-**5a**)$_2$ showing the characteristic binding motifs. e) Schematic representation of the capsules and the β-sheet binding motifs, illustrating the differences in the relative arrangement of the peptide chains. NMR monitoring of the exchange of hemispheres: ^{1}H NMR spectra of f) (L-**4b**)$_2$, g) (L-**4a**)$_2$, and h) (L-**4a**)$_2$ + (L-**4b**)$_2$ after 3 days and i) (L-**4a**)$_2$ + (D-**4b**)$_2$ after 3 days ($CDCl_3$/MeOH, 95:5, 300 K, 600 MHz). Chiral self-sorting during synthesis: ^{1}H NMR spectra of j) (L-**4a**)$_2$, k) (L-**4b**)$_2$, l) (L-**5a**)$_2$, m) the product of the reaction of **1** + L-**2a** + L-**2b**, n) the product of the reaction of **1** + L-**2a** + D-**2b**, o) the product of the reaction of **1** + L-**2b** + L-**3a**, and p) the product of the reaction of **1** + L-**2b** + D-**3a** (reaction conditions: 7 days, 70 °C, $CHCl_3$; NMR spectra recorded in $CDCl_3$, 300 K, 600 MHz).

Stability

To probe the stability of the dimers and the preference for chiral self-assembly, we analyzed two mixtures of capsules: (L-**4a**)$_2$+(L-**4b**)$_2$ (homochiral mixture) and (L-**4a**)$_2$+(D-**4b**)$_2$ (heterochiral mixture) in various media. In $CDCl_3$ at room temperature the ^{1}H NMR spectra remained unchanged in both cases, even after 7 days. Heating of the mixtures resulted in covalent scrambling, without a stage in which hybrid capsules made of two different hemispheres could be detected. To promote noncovalent exchange of the hemispheres, a small amount of a polar solvent was added (5% v/v MeOH). After 3 days, the equilibration process had led to the formation of a statistical mixture of hybrid capsules in the case of the homochiral mixture (Figure 2h), whereas no change was observed in the composition of the heterochiral mixture (Figure 2i). These results provide further evidence of the existence of dimeric forms in solution, even after the addition of polar solvents. They also indicate that homochiral dimers are highly preferred. Additionally, it should be noted that the self-assembled dimers have an unusually high kinetic stability in nonpolar solvent ($CDCl_3$) and relatively slow rates of hemisphere exchange (days) even after the addition of polar solvent.

Self-sorting

Various types of calixarene-based molecular capsules have shown self-sorting ability at the stage of their noncovalent self-assembly.[17] There are also several examples of the use of peptides to induce chiral self-sorting.[7a,b] However, a combination of noncovalent stabilization and the dynamic nature of chemical reactions that leads to effective self-sorting already at the stage of covalent synthesis of such capsules has only been reported by us for imine-based capsules.[9] In the present work, we performed a series of experiments to test the possibility of self-sorting for hydrazide substrates of different lengths and different chirality. For the reaction of **1** with a mixture of hydrazides of the same length but different chirality, for example, L-**2a**+D-**2b**, the exclusive formation of homochiral dimers was observed (Figure 2n and Figures S30–32 in the Supporting Information), in agreement with the previously observed preference towards homochiral dimers (by both X-ray diffraction and solution experiments). Effective chiral self-sorting also took place when racemic mixtures of dipeptidic hydrazides were used, for example, L-**3a**+D-**3a**, which led to the exclusive formation of homochiral dimers (see Figure S30f). However, when a mixture of hydrazides with the same length and the same chirality was used, for example, L-**2a**+L-**2b**, no sorting was observed (confirmed also by ^{13}C NMR, ESI-MS, and HPLC, Figure 2m and Figures S30–32). These results indicate that the chirality of the peptides governs the self-sorting process. The lack of self-sorting in the case of two peptides of the same chirality excludes the possibility that self-sorting is caused by interactions that are specific to these two particular peptides (e.g., C–H···π interactions between the side-chains of Val and Phe).

A plausible explanation for the amplification of homochiral capsules over heterochiral or mixed capsules may involve the concurrent involvement of various factors, for example, 1) the preference of acylhydrazone linkages towards the planar *E* conformation about the N–N bond (99.6% of the structures based on a CSD search and structures presented in this paper, see Figure S49 in the Supporting Information) and 2) the conformational preferences of peptides within a β-sheet binding motif according to the Ramachandran plot (especially for Val).[18]

Interestingly, no self-sorting was observed based on the length of the peptides. The reaction of **1** with a mixture of L-**2b**+L-**3a** (hydrazides of different length but the same chirality) led to a mixture of many products (Figure 2o). However, the reaction of **1** with a mixture of L-**2b**+D-**3a** (hydrazides of different length and different chirality) led to a well-defined mixture of only two products (L-**4b**)$_2$+(D-**5a**)$_2$ (Figure 2p). Thus, in the present case, only the chirality but not the length of the peptides plays a critical role in self-sorting. This is an intriguing observation because the complementarity of the binding motifs is the key factor in the self-sorting processes and results in the amplification of products composed of substrates of the same lengths. Complementarity is especially important for conformationally labile substrates, and, in fact, high-fidelity self-sorting based on length has been previously observed for imine-based peptidic capsules.[9] In the present case, the lack of length-dependence can be explained by a comparison of the binding motifs in capsules (L-**4b**)$_2$ and (D,L-**5a**)$_2$. In both capsules, the conserved binding motifs involve only the first amino acid residue in each strand. The presence of a second amino acid residue, Gly, in (D,L-**5a**)$_2$ does not lead to any significant elongation of the (D,L-**5a**)$_2$ capsule compared with (L-**4b**)$_2$, because it only forms additional interconnections between the "pairs of strands". However, the binding motifs in (L-**4b**)$_2$ and (D,L-**5a**)$_2$ are slightly different (Figure 2e). The difference can be minimized provided that a twist of the hemispheres with respect to each other is possible, resulting in a change in the binding motif from a 10- to a 14-membered hydrogen-bonded ring. Assisted by such a rotation, strands composed of amino acid derivatives and dipeptides could easily fit into the same binding motif, thereby leading to ineffective length-based self-sorting.

Complexation

The cavity volumes of the capsules were estimated by two different procedures. The calcVoid procedure[19] implemented in OLEX2[20] gave 801 Å^3 for (D-**4b**)$_2$ and 758 Å^3 for (D,L-**5a**)$_2$ (default solvent radius 1.42 Å, shrink truncation radius 1.42 Å). The Spaceball program[21] gave a value of 830 Å^3 for (D-**4b**)$_2$. Based on shape and size complementarity, we predicted that fullerene C_{60} (V=549 Å^3)[22] could fit into these cavities. Fullerene is also considered a good probe for monitoring the intrinsic open/close processes of capsules due to its size and lack of highly directional interactions with the external surfaces of capsules.

Complexation experiments in $CDCl_3$ did not show any traces of C_{60} encapsulation within the (L-**4a**)$_2$ or (L-**5a**)$_2$ capsules, even after several weeks (at RT and 70 °C). Complexes also failed to form after the addition of various amounts of MeOH, which was shown to promote capsule disassembly. However, when the reaction between **1** and hydrazide L-**2b** or L-**3a** was carried out in the presence of stoichiometric amounts of C_{60} or C_{70}, the quantitative formation of the respective complexes $C_{60}\subset$(L-**4b**)$_2$, $C_{60}\subset$(L-**5a**)$_2$, and $C_{70}\subset$(L-**5a**)$_2$ was observed. The formation of these complexes was unambiguously confirmed by clear new sets of signals in the ^{1}H and ^{13}C NMR and ESI-MS spectra (Figure 3a–g and Figures S35–S39 in the Supporting Information). After the formation of the complexes, the fullerenes were not released, even under conditions in which covalent scrambling is observed for free capsules ($CDCl_3$, 7 days, 70 °C).

These results indicate that the capsules have a high thermodynamic affinity towards the complexation of C_{60} and C_{70}; therefore the equilibrium is shifted towards the formation of complexes. However, the complexation of these guests is limited by a high kinetic barrier that precludes complexation inside capsules that have already been formed. But the complexation also does not proceed under the specific conditions in which covalent scrambling occurs (exchange of peptidic arms by the rupture of covalent bonds). It may be rationalized by assuming that covalent scrambling proceeds through a "one-at-a-time" mechanism, that is, at a single moment only one or two arms are removed while the rest of the capsule remains intact. Therefore, even though covalent scrambling occurs, the complexation or release of a large fullerene guest is still hampered, because it requires a considerable opening.

Although the complexation of fullerenes by the pre-assembled capsules did not proceed in solution, successful complexation could be achieved by using mechanochemical methods in the solid state. When a mixture of (L-**5a**)$_2$ and C_{60} was ball-milled for 1 hour, the complexation of C_{60} was observed. This result indicates that mechanochemical methods can be valuable tools for loading cargo into molecular capsules of high kinetic stability and that they are able to overcome kinetic barriers more effectively than in solution. Although mechanochemical encapsulation in micelles or liposomes is widely known, to the best of our knowledge, this is the first demonstration of mechanochemically induced encapsulation in molecular containers. The mechanism of action, as in many other mechanochemical processes, remains mostly unknown. However, we believe that explanations involving conformational changes and/or chemical reversibility under mechanochemical conditions due to local overheating are plausible.

The $C_{60}\subset$(L-**5a**)$_2$ complex was characterized by NMR spectroscopy and X-ray crystallography ($C_{60}\subset$(L-**5a**)$_2$ and $C_{60}\subset$(D-**5a**)$_2$ are enantiomeric but otherwise identical, see Figure S42 in the Supporting Information). In the ^{13}C NMR spectrum, the signal of encapsulated C_{60} appears as a sharp singlet shifted upfield by 2.0 ppm compared with the signal of the free guest

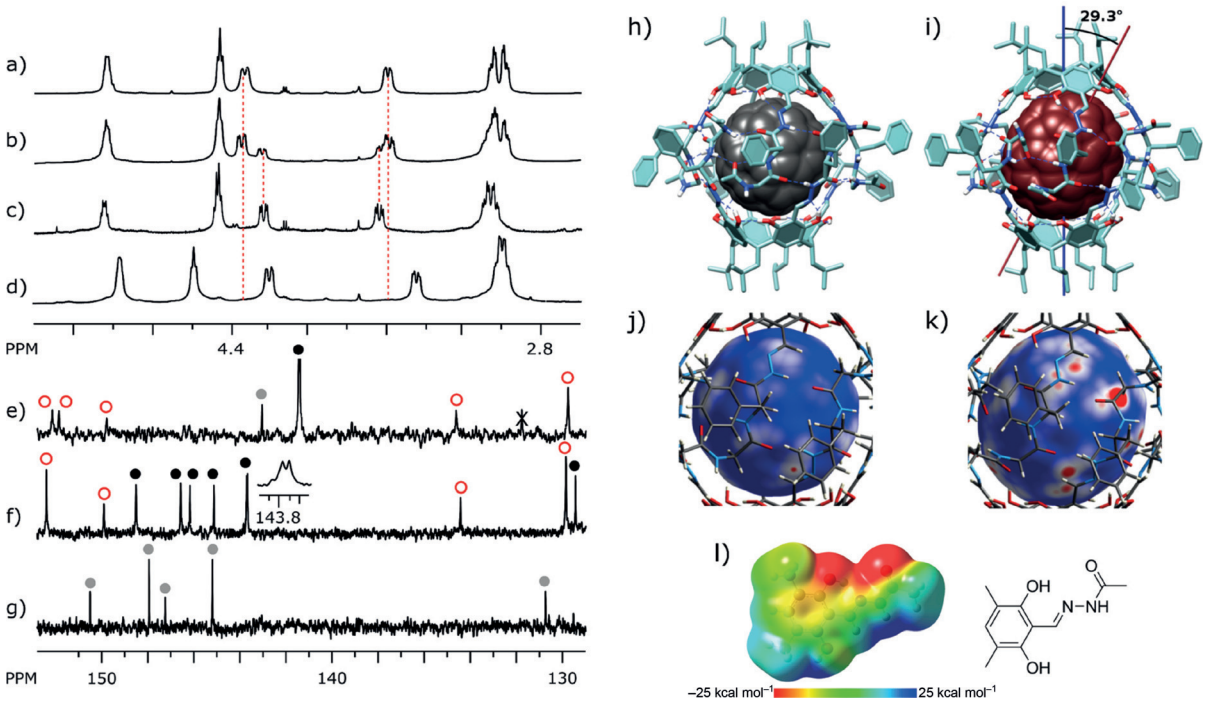

Figure 3. Complexation of fullerenes as shown by the ^{1}H (a–d) and ^{13}C (e–g) NMR spectra of a) (L-**5a**)$_2$, b) (L-**5a**)$_2$ + C_{60} after ball-milling, c) the product of the reaction of **1** + L-**3a** + C_{60}, d) the product of the reaction of **1** + L-**3a** + C_{70}, e) the product of the reaction of **1** + L-**3a** + C_{60}, f) the product of the reaction of **1** + L-**3a** + C_{70}, and g) C_{70} (○ capsules, ● free fullerene, ● encapsulated fullerene; $CDCl_3$, 600 MHz, 300 K). X-ray crystal structures of h, j) $C_{60}\subset$(D-**5a**)$_2$ and i, k) $C_{70}\subset$(D-**5a**)$_2$. The capsules are shown in stick representation and the fullerenes as van der Waals surfaces. The surfaces in (j,k) are color-coded for host–guest contacts after subtraction of the sum of the van der Waals radii: red: < 0 Å, white: = 0 Å, and blue: > 0 Å. The scale in the top and bottom panels is different for better visibility. The lines and angle in (i) show the mutual orientation of the principal axes of C_{70} and (D-**5a**)$_2$. l) Electrostatic potential mapped onto the total electron density isosurface of monomeric acylhydrazone (ab initio calculations, DFT B3LYP).

molecule (Figure 3e). The symmetry rules for C_{60} predict that all carbon atoms are homotopic, therefore, their chemical shifts are not differentiated upon encapsulation in a chiral capsule. The presence of a single signal for encapsulated C_{60} indicates that spinning of the fullerene within the capsule is fast on the NMR timescale. Despite this high rotational freedom in solution, in the solid state the guest molecule is perfectly ordered. The C_{60} molecule in the crystal structure was modeled and refined by using only two soft geometrical restraints (SADI for equivalence of the two unique C–C bonding distances), and the experimental electron density showed a well-resolved guest structure at full occupancy (Figure 3h and Figure S46). A van der Waals representation of the host–guest complex indicates that the geometric match is very good. However, the intramolecular distances between the host and guest molecules are systematically higher than the sum of the corresponding van der Waals radii (Figure 3j). Interestingly, the shortest distances are observed between C_{60} and the acylhydrazone groups (3.37 Å for $C_{fullerene}\cdots C{=}\mathbf{N}$).

In contrast to C_{60} complexation, the larger C_{70} guest complex could only just be detected, even after prolonged mechanochemical procedures. However, the fullerene molecule could be stoichiometrically complexed when the chemical reaction of **1** and L-**3a** was carried out in the presence of C_{70}. A comparison of the ^{13}C NMR spectra of free C_{70} and $C_{70}\subset$(L-**5a**)$_2$ shows significant complexation-induced shifts and symmetry changes. The ^{13}C NMR spectrum of $C_{70}\subset$(L-**5a**)$_2$ contains seven signals of equal intensity that have been attributed to complexed C_{70} (Figure 3f). The spectrum of free C_{70} contains five signals, two of which have an intensity twice that of the others, in accordance with the D_{5h} symmetry (in all solvents reported, including the spectrum in $CDCl_3$ recorded in this work, Figure 3g). The change in symmetry upon complexation can be attributed to the influence of the chiral environment. In chiral environments, enantiotopic carbon atoms (related by mirror planes) become diastereotopic and have different chemical shifts. Thus, the resulting symmetry of C_{70} in a chiral environment is D_5. In addition, the hindered rotation of C_{70} within the cavity would result in a further lowering of the symmetry of both the C_{70} guest and the capsule. Because such a symmetry reduction is not observed here, it must be concluded that the tumbling of C_{70} in the cavity is fast. The X-ray crystal structure of $C_{70}\subset$(D-**5a**)$_2$ shows a well resolved C_{70} molecule inside the cavity. Interestingly, the long axis of the C_{70} prolate spheroid is not aligned with the long axis of the capsule but has an approximate angle of tilt of 29° (angle in Figure 3i). A comparison of the three X-ray structures of (D-**5a**)$_2$, $C_{60}\subset$(D-**5a**)$_2$, and $C_{70}\subset$(D-**5a**)$_2$ indicates that the capsule skeletons have very similar geometries with a symmetry close to C_4 (deviations $<1\%$, see Figure S48 and movie in the Supporting Information). The association motif is conserved and the internal cavity volumes are similar in all structures. This indicates that the tilting of C_{70} inside the cavity is not caused by a distortion of the capsule shape, induced, for example, by packing forces or, indeed, by the guest molecule itself. The tilt must result, therefore, from favorable host–guest interactions. Indeed, analysis of the van der Waals contacts indicates that the host–guest distances are shorter for $C_{70}\subset$(L-**5a**)$_2$ than for $C_{60}\subset$(L-**5a**)$_2$ (Figure 3k). The shortest distances are observed between C_{70} and the acylhydrazone groups and glycine methylene hydrogen atoms of (L-**5a**)$_2$ (3.20 Å for $C_{fullerene}\cdots C{=}N$ and 2.38 Å for $C_{fullerene}\cdots H_{Gly}$).

The stoichiometric and quantitative complexation of fullerenes by peptide–resorcinarene capsules is non-intuitive due to the apparently different chemical nature of the host and guest molecules. Previously reported fullerene receptors were based mainly on extended complementary aromatic surfaces, for example, cyclotriveratrylenes and unmodified calixarenes, cycloparaphenylenes,[23] corannulenes,[24] phthalocyanines,[25] porphyrins,[26] anthracenes,[27] and even anthanthrene (six conjugated aromatic rings) macrocycles.[28] Even though large proteins have also been used to stabilize fullerenes in water, the stabilizing forces are largely unknown.[29] It has been postulated that the internal hydrophobic cavities of those proteins are mainly responsible for the interactions. In the present capsules, the shortest molecular interactions can be precisely determined, therefore they shed some light on the peptide–fullerene interactions. Surprisingly, the shortest intramolecular distances are observed not between the fullerenes and (as expected) the aromatic rings, but involve the acylhydrazone groups or the glycine methylene protons (part of the peptide backbone). To elucidate the participation of the acylhydrazone groups in the fullerene interactions, we performed ab initio DFT calculations (at the B3LYP level of theory) on a monomeric acylhydrazone unit (Figure 3l).[30] Calculations of the electrostatic potential indicated that a slightly negative potential extends from the aromatic ring to the acylhydrazone double bond. Therefore, interactions of this electron-rich fragment with fullerenes (which can be considered π acceptors) seem to be favorable. However, other factors may also contribute to the overall stabilization of these complexes (e.g., solvophobic interactions, as was previously suggested for the complexation of C_{60} in naphthalenediimide nanotubes).[31]

Conclusion

A series of molecular capsules based on amino acid and peptide derivatives attached to macrocyclic scaffolds have been synthesized. The dynamic character of the acylhydrazone moiety, used as the linker, and effective self-assembly enabled highly selective syntheses of the capsules from racemic mixtures of hydrazides by high-fidelity chiral self-sorting. The capsules have greatly enhanced thermodynamic and kinetic stability compared with the previously reported capsules based on imine linkers. The stability enhancement stems from the robustness of the noncovalent binding motif and from the higher hydrolytic stability of the covalent linker. Although the capsules retain their dynamic character, thereby allowing processes such as chiral self-sorting and chiral self-assembly to occur with high precision, other processes, like complexation by pre-assembled capsules are markedly hampered. Therefore, the encapsulation of fullerene buckyballs, which match the size and shape of the cavity of the pre-assembled capsules, cannot be accomplished in solution. However, as conclusively demonstrated in this work, the complexation energy barrier

can be successfully overcome by utilizing the reversible character of the covalent bonds, or by mechanochemical methods.

Experimental Section

The use of $CDCl_3$ or $CHCl_3$ as solvent was dictated by the experimental conditions (e.g., in situ experiments in NMR tubes). The use of deuterated solvent had no influence on the properties of the investigated capsules.

Synthesis of capsules: Tetraformylresorcin[4]arene **1**[10] (0.05 mmol, 41 mg) and the respective hydrazide **2a**–**3b** (0.2 mmol) were dissolved in $CHCl_3$ (2 mL) in a sealed pressure vial. The mixture was heated at 70 °C for 20 h. Then the reaction mixture was cooled down and filtered. The solution was evaporated under reduced pressure and vacuum-dried. Acylhydrazones **4a**–**5b** (as noncovalent dimers (L-**4a**)$_2$–(D-**5b**)$_2$) were obtained as yellow solids in yields of 92–98%.

Scrambling experiment: (L-**4a**)$_2$ (0.006 mmol, 9.8 mg) and (L-**4b**)$_2$ (0.006 mmol, 8.6 mg) were dissolved in $CDCl_3$ (1 mL). The mixture was stirred at 70 °C for 7 days in a sealed pressure vial. After cooling, the sample was analyzed by ^{1}H NMR spectroscopy and ESI-MS. The presence of mixed products (scrambled) was detected.

Self-sorting experiments: Tetraformylresorcin[4]arene **1** (0.05 mmol, 41 mg) and two different hydrazides (0.1 mmol each) were dissolved in $CHCl_3$ (2 mL) in a sealed pressure vial. The reaction mixture was stirred at 70 °C for 7 days. Then, the mixture was cooled down and filtered. The solution was evaporated under reduced pressure. The solid was analyzed by ^{1}H and ^{13}C NMR spectroscopy.

Complexation of fullerenes using mechanochemical methods: (L-**5a**)$_2$ (0.005 mmol, 16.4 mg) and C_{60} (0.005 mmol, 3.6 mg) were placed in a grinding vial. The sample was ball-milled at a milling rate of 500 min^{-1} for 1 h. Then the sample was dissolved in $CDCl_3$ (1 mL) and filtered. The products were analyzed by NMR spectroscopy. The complexation of C_{70} was studied by an analogous procedure. The partial complexation of C_{60} (ca. 30%) and C_{70} (ca. 5%) was detected.

Complexation of fullerenes during chemical reaction: Tetraformylresorcin[4]arene **1** (0.02 mmol, 16.5 mg), L-**3a** (0.08 mmol, 22.2 mg), and C_{60} (0.01 mmol, 7.2 mg) were dissolved in $CHCl_3$ (2 mL) in a sealed pressure vial. The reaction mixture was stirred at 70 °C for 4 days. The mixture was cooled down and filtered. Then the solution was evaporated under reduced pressure. The products were analyzed by NMR spectroscopy. The complexation of C_{70} was studied by an analogous procedure. Hydrazides D-**3a** and L-**2b** were tested in a similar way. In all cases, the quantitative formation of stoichiometric complexes was detected.

X-ray structure determination: Single crystals of (D-**4b**)$_2$ were grown by the slow diffusion of ethanol vapor into a chloroform solution. Single crystals of (D,L-**5a**)$_2$ were grown by the slow diffusion of isopropanol vapor into a chloroform solution. Single crystals of $C_{60}\subset$(L-**5a**)$_2$ were grown by the slow diffusion of acetonitrile vapor into a chloroform solution. Single crystals of $C_{70}\subset$(L-**5a**)$_2$ were grown by the slow diffusion of methanol vapor into a chloroform solution. X-ray measurements were carried out by using an Agilent SuperNova diffractometer ($Cu_{K\alpha}$ radiation) for (D-**4b**)$_2$ and $C_{70}\subset$(L-**5a**)$_2$ and at the MaxLab II synchrotron beamline 1911-3 (Lund, Sweden) at $\lambda = 0.8000$ Å for (D,L-**5a**)$_2$ and $C_{60}\subset$(L-**5a**)$_2$. The structures were solved by using SHELXS[32] (the capsules) or by molecular replacement using the PHASER[33] module of the CCP4 suite[34] and capsule skeletons as molecular probes (in the case of fullerene complexes).[35] The structures were refined by using SHELXL with anisotropic displacement parameters for all non-hydrogen atoms. All hydrogen atoms were included at geometrically predicted coordinates. For (D,L-**5a**)$_2$, $C_{60}\subset$(L-**5a**)$_2$, and $C_{70}\subset$(L-**5a**)$_2$, stereochemical restraints were applied to the bond lengths in the peptidic chains and the fullerene molecules. Soft restraints were also applied to thermal parameters as necessary (in disordered regions). Highly disordered solvent molecules were removed from the electron density by means of the Solvent Masking procedure in OLEX2.[20]

CCDC 1060617 ((D-**4b**)$_2$), 1060618 ((D,L-**5a**)$_2$), 1060619 ($C_{60}\subset$(L-**5a**)$_2$), and 1060620 ($C_{70}\subset$(L-**5a**)$_2$) contain the supplementary crystallographic data for this paper. These data are provided free of charge by The Cambridge Crystallographic Data Centre.

Acknowledgements

This work was supported by the Foundation for Polish Science (A.S. and H.J., grant POMOST/2011-4/10), the National Science Center (M.J. and M.G., grant 2013/10M/NZ1/00251) and the Wroclaw Centre for Networking and Supercomputing (grant no. 299). The research leading to these results was funded by the European Community's Seventh Framework Programme (FP7/2007-2013) under BioStruct-X (grant agreement no. 283570). We thank MAX IV Laboratory in Lund for the allocation of synchrotron radiation beamtime. We would like to acknowledge Prof. Kinga Suwińska for her help with in-house X-ray data collection, and Dr. Michał Michalak and Paweł Czerwiński for their assistance with HPLC and ball-milling experiments, respectively.

Keywords: chirality · fullerenes · mechanochemistry · peptide mimics · supramolecular chemistry

[1] a) D. G. Fatouros, D. A. Lamprou, A. J. Urquhart, S. N. Yannopoulos, I. S. Vizirianakis, S. Zhang, S. Koutsopoulos, *ACS Appl. Mater. Interfaces* **2014**, *6*, 8184–8189; b) J. J. Panda, V. S. Chauhan, *Polym. Chem.* **2014**, *5*, 4418–4431.

[2] a) J. B. Matson, S. I. Stupp, *Chem. Commun.* **2012**, *48*, 26–33; b) H. Hosseinkhani, P. D. Hong, D. S. Yu, *Chem. Rev.* **2013**, *113*, 4837–4861; c) R. Ravichandran, M. Griffith, J. Phopase, *J. Mater. Chem. B* **2014**, *2*, 8466–8478.

[3] D. Li, E. M. Jones, M. R. Sawaya, H. Furukawa, F. Luo, M. Ivanova, S. A. Sievers, W. Wang, O. M. Yaghi, C. Liu, D. S. Eisenberg, *J. Am. Chem. Soc.* **2014**, *136*, 18044–18051.

[4] G. W. Collie, K. P. Ziach, C. M. Lombardo, J. Fremaux, F. Rosu, M. Decossas, L. Mauran, O. Lambert, V. Gabelica, C. D. Mackereth, G. Guichard, *Nat. Chem.* **2015**, *7*, 871–878.

[5] B. E. I. Ramakers, J. C. M. Hest, D. W. P. M. van Löwik, *Chem. Soc. Rev.* **2014**, *43*, 2743–2756.

[6] a) L. Adler-Abramovich, E. Gazit, *Chem. Soc. Rev.* **2014**, *43*, 6881–6893; b) H. Cui, M. J. Webber, S. I. Stupp, *Biopolymers* **2010**, *94*, 1–18; c) S. Fleming, R. V. Ulijn, *Chem. Soc. Rev.* **2014**, *43*, 8150–8177.

[7] a) N. Ponnuswamy, F. B. L. Cougnon, J. M. Clough, G. Dan Pantos, J. K. M. Sanders, *Science* **2012**, *338*, 783–785; b) N. Ponnuswamy, F. B. L. Cougnon, G. Dan Pantoş, J. K. M. Sanders, *J. Am. Chem. Soc.* **2014**, *136*, 8243–8251; c) J. M. A. Carnall, C. A. Waudby, A. M. Belenguer, M. C. A. Stuart, J. J. P. Peyralans, S. Otto, *Science* **2010**, *327*, 1502–1506; d) J. W. Sadownik, R. V. Ulijn, *Curr. Opin. Biotechnol.* **2010**, *21*, 401–411; e) R. L. Schoch, L. E. Kapinos, R. Y. H. Lim, *Proc. Natl. Acad. Sci. USA* **2012**, *109*, 16911–16916; f) A. Pal, M. Malakoutikhah, G. Leonetti, M. Tezcan, M. Colomb-Delsuc, V. D. Nguyen, J. van der Gucht, S. Otto, *Angew. Chem. Int. Ed.* **2015**, *54*, 7852–7856; *Angew. Chem.* **2015**, *127*, 7963–7967; g) A. Moure, S. V. Luis, I. Alfonso, *Chem. Eur. J.* **2012**, *18*, 5496–5500;

h) Y. Krishnan-Ghosh, S. Balasubramanian, *Angew. Chem. Int. Ed.* **2003**, *42*, 2171 – 2173; *Angew. Chem.* **2003**, *115*, 2221 – 2223.

[8] a) T. Friščić, *Chem. Soc. Rev.* **2012**, *41*, 3493 – 3510; b) D. W. R. Balkenende, S. Coulibaly, S. Balog, Y. C. Simon, G. L. Fiore, C. Weder, *J. Am. Chem. Soc.* **2014**, *136*, 10493 – 10498.

[9] H. Jędrzejewska, M. Wierzbicki, P. Cmoch, K. Rissanen, A. Szumna, *Angew. Chem. Int. Ed.* **2014**, *53*, 13760 – 13764; *Angew. Chem.* **2014**, *126*, 13980 – 13984.

[10] M. Grajda, M. Wierzbicki, P. Cmoch, A. Szumna, *J. Org. Chem.* **2013**, *78*, 11597 – 11601.

[11] G. R. L. Cousins, S. A. Poulsen, J. K. M. Sanders, *Chem. Commun.* **1999**, 1575 – 1576.

[12] a) R. T. S. Lam, A. Belenguer, S. L. Roberts, C. Naumann, T. Jarrosson, S. Otto, J. K. M. Sanders, *Science* **2005**, *308*, 667 – 669; b) F. B. L. Cougnon, J. K. M. Sanders, *Acc. Chem. Res.* **2012**, *45*, 2211 – 2221.

[13] a) J. A. Prescher, C. R. Bertozzi, *Nat. Chem. Biol.* **2005**, *1*, 13 – 21; b) V. T. Bhat, A. M. Caniard, T. Luksch, R. Brenk, D. J. Campopiano, M. F. Greaney, *Nat. Chem.* **2010**, *2*, 490 – 497.

[14] a) A. Dirksen, S. Dirksen, T. M. Hackeng, P. E. Dawson, *J. Am. Chem. Soc.* **2006**, *128*, 15602 – 15603; b) P. Crisalli, E. T. Kool, *J. Org. Chem.* **2013**, *78*, 1184 – 1189.

[15] a) Y. S. Park, J. Park, K. Paek, *Chem. Commun.* **2015**, *51*, 6006 – 6009; b) Y. S. Park, J. Park, K. Paek, *Chem. Commun.* **2013**, *49*, 6316 – 6318.

[16] a) N. Galić, I. Brođanac, D. Kontrec, S. Miljanić, *Spectrochim. Acta Part A* **2013**, *107*, 263 – 270; b) A. Manimekalai, N. Saradhadevi, A. Thiruvalluvar, *Spectrochim. Acta Part A* **2010**, *77*, 687 – 695; c) V. I. Minkin, A. V. Tsukanov, A. D. Dubonosov, V. A. Bren, *J. Mol. Struct.* **2011**, *998*, 179 – 191.

[17] a) H. Gan, B. C. Gibb, *Chem. Commun.* **2012**, *48*, 1656 – 1658; b) M. Chas, G. Gil-Ramirez, P. Ballester, *Org. Lett.* **2011**, *13*, 3402 – 3405; c) M. Chas, G. Gil-Ramirez, E. C. Escudero-Adan, J. Benet-Buchholz, P. Ballester, *Org. Lett.* **2010**, *12*, 1740 – 1743; d) D. Ajami, J. L. Hou, T. J. Dale, E. Barrett, J. Rebek, *Proc. Natl. Acad. Sci. USA* **2009**, *106*, 10430 – 10434; e) E. S. Barrett, T. J. Dale, J. Rebek, *J. Am. Chem. Soc.* **2008**, *130*, 2344 – 2350; f) D. Braekers, C. Peters, A. Bogdan, Y. Rudzevich, V. Bohmer, J. F. Desreux, *J. Org. Chem.* **2008**, *73*, 701 – 706; g) A. Wu, L. Isaacs, *J. Am. Chem. Soc.* **2003**, *125*, 4831 – 4835.

[18] S. Hovmöller, T. Zhou, T. Ohlson, *Acta Crystallogr. Sect. D* **2002**, *58*, 768 – 776.

[19] B. Rees, L. Jenner, M. Yusupov, *Acta Crystallogr. Sect. D* **2005**, *61*, 1299 – 1301.

[20] O. V. Dolomanov, L. J. Bourhis, R. J. Gildea, J. A. K. Howard, H. Puschmann, *J. Appl. Crystallogr.* **2009**, *42*, 339 – 341.

[21] M. Chwastyk, M. Jaskolski, M. Cieplak, *FEBS J.* **2014**, *281*, 416 – 429.

[22] G. B. Adams, M. O'Keeffe, R. S. Ruoff, *J. Phys. Chem.* **1994**, *98*, 9465 – 9469.

[23] T. Iwamoto, Y. Watanabe, H. Takaya, T. Haino, N. Yasuda, S. Yamago, *Chem. Eur. J.* **2013**, *19*, 14061 – 14068.

[24] A. S. Filatov, M. V. Ferguson, S. N. Spisak, B. Li, C. F. Campana, M. A. Petrukhina, *Cryst. Growth Des.* **2014**, *14*, 756 – 762.

[25] I. Sánchez-Molina, C. G. Claessens, B. Grimm, D. M. Guldiand, T. Torres, *Chem. Sci.* **2013**, *4*, 1338 – 1344.

[26] X. Fang, Y. Z. Zhu, J. Y. Zheng, *J. Org. Chem.* **2014**, *79*, 1184 – 1191.

[27] N. Kishi, M. Akita, M. Yoshizawa, *Angew. Chem. Int. Ed.* **2014**, *53*, 3604 – 3607; *Angew. Chem.* **2014**, *126*, 3678 – 3681.

[28] T. Matsuno, S. Sato, R. Iizuka, H. Isobe, *Chem. Sci.* **2015**, *6*, 909 – 916.

[29] a) H. Wu, L. Lin, P. Wang, S. Jiang, Z. Dai, X. Zou, *Chem. Commun.* **2011**, *47*, 10659 – 10661; b) M. Calvaresi, F. Arnesano, S. Bonacchi, A. Bottoni, V. Calò, S. Conte, G. Falini, S. Fermani, M. Losacco, M. Montalti, G. Natile, L. Prodi, F. Sparla, F. Zerbetto, *ACS Nano* **2014**, *8*, 1871 – 1877.

[30] Gaussian 09, Revision B.01, M. J. Frisch, G. W. Trucks, H. B. Schlegel, G. E. Scuseria, M. A. Robb, J. R. Cheeseman, G. Scalmani, V. Barone, B. Mennucci, G. A. Petersson, H. Nakatsuji, M. Caricato, X. Li, H. P. Hratchian, A. F. Izmaylov, J. Bloino, G. Zheng, J. L. Sonnenberg, M. Hada, M. Ehara, K. Toyota, R. Fukuda, J. Hasegawa, M. Ishida, T. Nakajima, Y. Honda, O. Kitao, H. Nakai, T. Vreven, J. A. Montgomery, Jr., J. E. Peralta, F. Ogliaro, M. Bearpark, J. J. Heyd, E. Brothers, K. N. Kudin, V. N. Staroverov, R. Kobayashi, J. Normand, K. Raghavachari, A. Rendell, J. C. Burant, S. S. Iyengar, J. Tomasi, M. Cossi, N. Rega, J. M. Millam, M. Klene, J. E. Knox, J. B. Cross, V. Bakken, C. Adamo, J. Jaramillo, R. Gomperts, R. E. Stratmann, O. Yazyev, A. J. Austin, R. Cammi, C. Pomelli, J. W. Ochterski, R. L. Martin, K. Morokuma, V. G. Zakrzewski, G. A. Voth, P. Salvador, J. J. Dannenberg, S. Dapprich, A. D. Daniels, Ö. Farkas, J. B. Foresman, J. V. Ortiz, J. Cioslowski, and D. J. Fox, Gaussian, Inc., Wallingford CT, **2009**.

[31] N. Ponnuswamy, G. D. Pantoş, M. M. J. Smulders, J. K. M. Sanders, *J. Am. Chem. Soc.* **2012**, *134*, 566 – 573.

[32] G. M. Sheldrick, *Acta Crystallogr. Sect. A* **2008**, *64*, 112 – 122.

[33] A. J. McCoy, R. W. Grosse-Kunstleve, P. D. Adams, M. D. Winn, L. C. Storoni, R. J. Read, *J. Appl. Crystallogr.* **2007**, *40*, 658 – 674.

[34] M. D. Winn, C. C. Ballard, K. D. Cowtan, E. J. Dodson, P. Emsley, P. R. Evans, R. M. Keegan, E. B. Krissinel, A. G. W. Leslie, A. McCoy, *Acta Crystallogr. Sect. D* **2011**, *67*, 235 – 242.

[35] M. Wierzbicki, M. Gilski, K. Rissanen, M. Jaskolski, A. Szumna, *CrystEngComm* **2014**, *16*, 3773 – 3780.

Received: November 5, 2015
Published online on January 25, 2016